

# Actively mode-locked laser in nanophotonic lithium niobate

Qiushi Guo<sup>1</sup>, Ryoto Sekine<sup>1</sup>, James A. Williams<sup>1</sup>, Benjamin Gutierrez<sup>2</sup>, Robert M. Gray<sup>1</sup>, Luis Ledezma<sup>1,3</sup>, Luis Costa<sup>1</sup>, Selina Zhou<sup>1</sup>, Alireza Marandi<sup>1</sup>

<sup>1</sup> Department of Electrical Engineering, California Institute of Technology, Pasadena, California 91125, USA

<sup>2</sup> Department of Applied Physics, California Institute of Technology, Pasadena, California 91125, USA

<sup>3</sup> Jet Propulsion Laboratory, California 91109, USA

marandi@caltech.edu

**Abstract:** We report an electrically pumped hybrid lithium niobate/III-V actively mode-locked laser. The laser emits 4.8 ps pulses at 10.17 GHz around 1065 nm with high peak power of  $\sim 1$  W. © 2023 The Author(s)

A mode-locked laser (MLL) emits a periodic train of ultrashort pulses with high peak power with low timing jitter. Since its first realization, MLLs have enabled numerous optical technologies such as nonlinear optical signal generation [1], optical atomic clocks [2], optical frequency combs and spectroscopic sensing systems [3]. The chip-scale integration of MLLs can revolutionize the field of ultrafast photonics by transforming lab-based tabletop systems into power-efficient portable light sources for more widespread applications. However, so far, the performance of integrated MLLs have been far behind their table-top counterparts, lacking the required peak intensities and degrees of controllability required for ultrafast optical systems [4]. Recently, thin-film lithium niobate (TFLN) has emerged as a promising integrated photonic platform due to its strong  $\chi^{(2)}$  nonlinearity and excellent electro-optic (EO) properties [5]. It is established that many of the ultrafast optical functionalities can be realized in TFLN with orders of magnitude lower requirements in peak powers and pulse energies [6–9]. Developing MLLs that are amenable to integration with TFLN promises new nonlinear and ultrafast photonic architectures with unprecedented performances.

Here we report the first electrically pumped actively MLL based on an integrated hybrid III-V/TFLN platform. In our MLL (Fig. 1a), a gain section based on a single angled facet III-V semiconductor gain chip (gain chip) operating around 1064 nm is butt-coupled to an integrated TFLN EO phase modulator. A Fabry-Perot laser cavity configuration is formed between the reflective facet of on the left end of the gain chip and the integrated broadband loop mirror on the right end of the TFLN phase modulator. The length of the TFLN waveguide is carefully designed to ensure a laser cavity free spectral range (FSR) of  $\sim 10$  GHz. At the coupling region, the TFLN waveguide is tapered out to 10  $\mu$ m in width, which ensures maximal overlap with the optical mode produced by the gain chip and a minimum coupling loss of  $\sim 1.6$  dB. Fig. 1b shows the microscope image of the actively MLL when the gain chip is electrically pumped. Inside the laser cavity, we can even observe green light (the second harmonic of 1064 nm light), indicating a high intra-cavity power around 1064 nm and good coupling between the two chips. As shown in Fig. 1c, the laser offers a very low threshold current of  $\sim 22$  mA and the laser output average power is more than 40 mW on the chip when the driving current is greater than 180 mA.

To test the MLL, we apply  $\sim 280$  mW RF power to the left end of the E-O phase modulator traveling wave electrodes (TWE) by the RF probe, and the right end of the TWE is terminated by a 50  $\Omega$  load resistor. We investigate the operating regimes of the MLL by simultaneously collecting the laser output spectra, the intensity autocorrelation of the laser output, and the heterodyne beat notes between two neighboring laser emission lines and a narrow-linewidth reference CW laser. In the measurement, the gain chip is pumped with 185.2 mA driving current, which leads to 43 mW output average power on chip. As shown in Fig. 1d, when we widely scan the RF driving frequency ( $f_{\text{drive}}$ ) from 9.5 to 11 GHz, the laser output exhibits a clear spectral broadening within the range of 10.1 to 10.4 GHz. Meanwhile, within this frequency range, two distinct intensity autocorrelation peaks separated by 98 ps emerge, indicating that optical pulses are formed in this regime (Fig. 1e). When tuning the  $f_{\text{drive}}$  between 10.1 to 10.4 GHz, we found that the heterodyne beat notes become the narrowest around 10.17 GHz. This suggests that 10.17 GHz is the closest frequency to the cavity FSR. At this frequency, all the laser emission modes are well phase-locked. As shown in Fig. 1f, at  $f_{\text{drive}} = 10.17$  GHz, the linewidths of the two beat notes at 3.68 GHz and 6.49 GHz are both  $\sim 4.7$  MHz, which is resulting from the drift of carrier envelop offset frequency ( $f_{\text{ceo}}$ ) of the laser. At  $f_{\text{drive}} = 10.17$  GHz, we collect the intensity autocorrelation of the laser output as shown in Fig. 1g. By assuming a Gaussian pulse shape, we extrapolate that the output optical pulse length is 4.81 ps (5.03 ps) with (without) the dispersion compensation by an external pulse shaper. Moreover, the mode-locking remains operational up to 200 mA, corresponding to on-chip average of 52 mW. Based on these results, the maximum

pulse energy is 5 pJ and the maximum peak power is  $\sim 0.9$  W, representing the highest peak power reported in waveguide-integrated MLLs. Looking forward, our TFLN-integrated MLL can drive many of the  $\chi^{(2)}$  nonlinear photonic processes in TFLN and enable integrated ultrafast photonic systems.

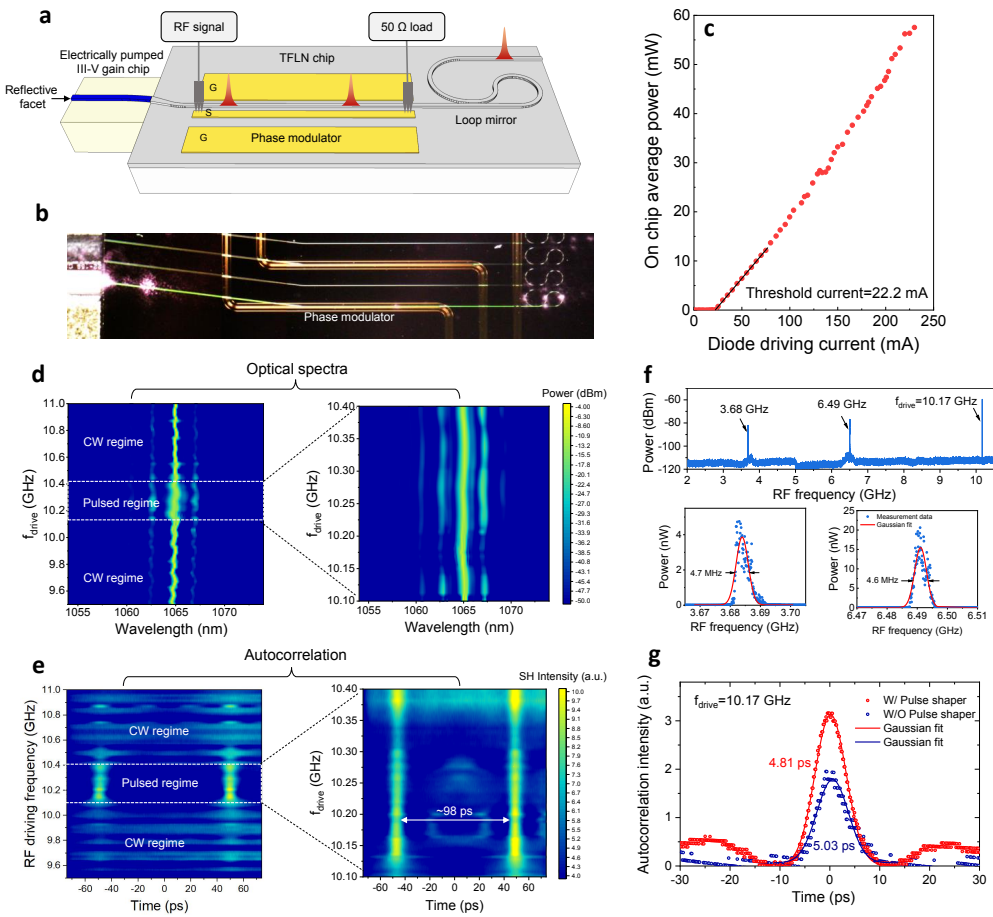


Fig. 1. (a) Schematic of an integrated TFLN MLL. (b) Optical microscope image of the integrated MLL when operating. (c) Measured on-chip average output power as a function of the laser driving current. (d) The optical spectrum of the MLL output as a function of the RF driving frequency ( $f_{\text{drive}}$ ). (e) Intensity autocorrelation trace of the MLL output as a function of the  $f_{\text{drive}}$ . (f) Heterodyne beat notes between the one of the laser lines near the center of the spectrum and a stable, narrow-linewidth reference CW laser. (g) Intensity autocorrelation measured at  $f_{\text{drive}} = 10.17$  GHz with (red) and without (blue) the external pulse shaper.

## References

1. J. M. Dudley and J. R. Taylor (Cambridge University Press, 2010).
2. S. A. Diddams, T. Udem, J. Bergquist, E. Curtis, R. Drullinger, L. Hollberg, W. M. Itano, W. Lee, C. Oates, K. Vogel *et al.*, *Science* **293**, 825–828 (2001).
3. N. Picqué and T. W. Hänsch, *Nat. Photonics* **13**, 146–157 (2019).
4. M. L. Davenport, S. Liu, and J. E. Bowers, *Photonics Res.* **6**, 468–478 (2018).
5. D. Zhu, L. Shao, M. Yu, R. Cheng, B. Desiatov, C. Xin, Y. Hu, J. Holzgrafe, S. Ghosh, A. Shams-Ansari *et al.*, *Adv. Opt. Photonics* **13**, 242–352 (2021).
6. Q. Guo, R. Sekine, L. Ledezma, R. Nehra, D. J. Dean, A. Roy, R. M. Gray, S. Jahani, and A. Marandi, *Nat. Photonics* **16**, 625–631 (2022).
7. L. Ledezma, A. Roy, L. Costa, R. Sekine, R. Gray, Q. Guo, R. M. Briggs, and A. Marandi, arXiv preprint arXiv:2203.11482 (2022).
8. L. Ledezma, R. Sekine, Q. Guo, R. Nehra, S. Jahani, and A. Marandi, *Optica* **9**, 303–308 (2022).
9. R. Nehra, R. Sekine, L. Ledezma, Q. Guo, R. M. Gray, A. Roy, and A. Marandi, *Science* **377**, 1333–1337 (2022).